Arch. Metall. Mater. **69** (2024), 4, 1669-1674

DOI: https://doi.org/10.24425/amm.2024.151439

D. FACHIKOVA[1*], G. ILIEVA[1]

COMPARISON OF CORROSION BEHAVIOR OF TWO STAINLESS STEELS FOR MEDICAL APPLICATIONS

Various materials are used in medicine and the main requirement is their biocompatibility, including corrosion resistance. In addition to destroying materials, the products released during corrosion can cause adverse reactions in the human body. Corrosion testing of any material proposed for biomaterials should therefore be conducted in a model or controlled environment similar to that of the human body.

In this work, the results obtained in the study of high nitrogen stainless steel (HNS) as a material for the fabrication of implants are presented and compared with the results for classical Cr-Ni stainless steel, in analogous environments and conditions.

The tests were carried out in Ringer's and Hartmann's solutions, at specified concentrations, temperatures and pH values. A three-electrode glass cell was used under open air conditions. The following electrochemical methods were used: open circuit potential (OCP) – time measurement, cyclic potentiodynamic and potentiostatic polarizations.

By means of light and scanning electron microscopy, surface changes were determined after exposing the steel specimens to the experimental media. The surface of the samples was also examined by EDX analysis to determine the nature of the corrosion products formed.

From the results obtained, it was found that HNS-steel has higher resistance than Cr-Ni-steel in the model solutions studied.

Keyword: Biocompatibility; stainless steels; high nitrogen steels; corrosion; electrochemical method

1. Introduction

The main requirement for the various artificial and synthetic engineering materials used for orthopaedic purposes in medicine is their biocompatibility, high mechanical properties and last but not least their corrosion resistance. Substances released during corrosion can cause adverse reactions in the human body, including poisoning. Therefore, corrosion testing of any material proposed for biomaterials must be conducted in a model or controlled environment similar to that of the human body [1-3].

Many metals (Ti, Ta, Co, Mn and its alloys), stainless steels for instance, are widely used in surgical operations as materials of implants [4-9]. Therefore, corrosion tests of new materials suggested as implants should be performed in controlled media simulating human body fluids prior to final implementations.

The use of stainless steels as orthopedic materials is due to its relatively low value in comparison with the other metals and alloys. The classic austenitic stainless steels exhibit good mechanical and corrosion properties but its Ni content provokes toxicity in the human body [10]. To avoid this problem high nitrogen stainless steels (HNS) such as 314L [11] have been developed to replace Ni-containing materials for implants. The interest about the corrosion resistance of HNS as orthopedic materials is provoked by the fact that stems made of Orthinox (high nitrogen stainless steel but still containing nickel), for instance, occupies 70% of the hip prostheses market and it is necessary to be replaced by non-toxic materials [12].

In the presented work, the results obtained from the study of the behavior, the nature of failure and the composition of the products, in the corrosion of two austenitic stainless steels Cr18Ni9 and Cr18Mn12N in two saline solutions: Ringer's infusion solution and Hartmann's lactate infusion solution are presented.

2. Experiment

Two austenitic stainless steels: the conventional Cr18Ni9 and the newly developed HNS Cr18Mn12N, were investigated in Ringer's infusion and Hartmann's lactate infusion solutions. The chemical composition of the two steels studied is presented in TABLE 1.

[1] UNIVERSITY OF CHEMICAL TECHNOLOGY AND METALLURGY, FACULTY OF CHEMICAL TECHNOLOGY, 8 KLIMENT OHRIDSKI BLVD., 1756 SOFIA, BULGARIA

* Corresponding author: dimkaivanova@uctm.edu

TABLE 1

The chemical composition (wt.% and at.%) of the stainless steels

Steel		Cr	Ni	Mn	C	N	Si	P	S
Cr18Mn12N	wt.%	16.50	0.05	12.00	0.04	0.61	0.36	0.011	0.023
	at.%	17.07	0.05	11.74	0.16	2.37	0.70	0.02	0.005
Cr18Ni9	wt.%	17.49	9.37	1.29	0.05	—	0.52	0.022	0.009
	at.%	18.74	8.85	1.23	0.23	—	1.03	0.04	0.016

TABLE 2

The chemical composition (g l^{-1}) of the tested solutions

Solution	Composition of the solution, g l^{-1}						
Ringer's	NaCl	KCl	$CaCl_2.2H_2O$	$Na_2HPO_4.2H_2O$	$NaHCO_3$	Urea,	Dist.H_2O
	6.8	0.40	0.2	0.143	2.2	1.00	1000
Hartmann's lactate	NaCl	KCl	$CaCl_2.2H_2O$	$Na_2HPO_4.2H_2O$	$NaHCO_3$	Sodium lactate	Dist.H_2O
	6.00	0.40	0.40	—	—	3.12	1000

Working specimens in the shape of a disc with a diameter of 7.981 mm and a working area of 0.5 cm^2 were made from the steel's billets. The specimens were electrically wired with copper conductor, then were placed in a glass ring and insulated with acrylic resin [13]. All tests were conducted in a conventional 3 – electrode cell, in open air conditions at 37°C, with a platinum counter electrode and a SCE, as a reference one. The electrochemical cell and working specimen are shown in Fig. 1. In addition, samples of square plates (10×10 mm) are used for the physical analyzes.

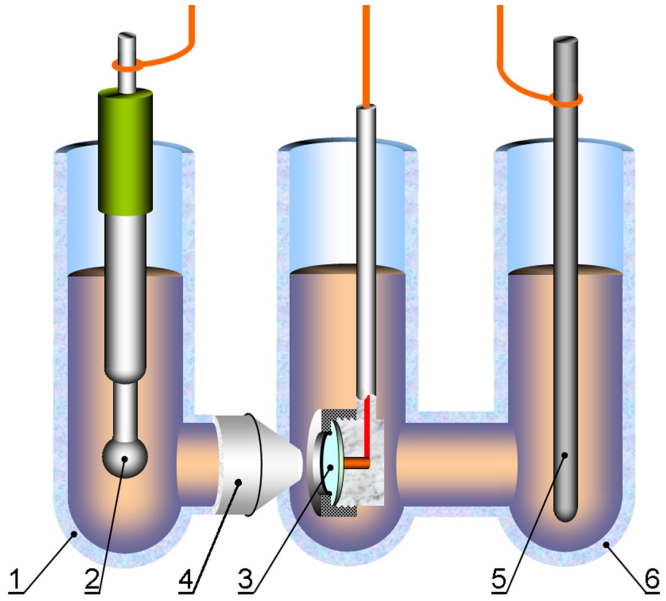

Fig. 1. Electrochemical cell for measurements: 1, 6 – glass cell; 2 – reference electrode (SCE); 3 – working electrode (WE); 4 – Luggin-Haber capillary; 5 – counter electrode (CE)

2.1. Solutions and working conditions

The chemical composition of the two environments in which were conducted the studies is presented in TABLE 2.

The pH and conductivity values σ, mS cm^{-1} of the solutions are shown in TABLE 3.

TABLE 3

The parameters of the solutions, at 37°C

Solution	pH	σ, mS cm^{-1}
Ringer's infusion solution	5.61	13.23
Hartmann's lactate infusion solution	6.24	11.05

Before each experiment, the working surface of the electrodes was treated with sandpaper (P280 to P1200), then washed with water and dried. Next, degrease in a mixture of alcohol and ether (1:1), wash with distilled water and dry.

2.2. Methods of investigation

2.2.1. Electrochemical methods

Open circuit potential measurement. When metals are immersed in liquid electrolyte media, on Me-medium interface a non-equilibrium or so called corrosion potentials, are established. The latter are not strictly indicative of the resistance of metals, but their values and variation with time provide sufficient information about the nature of the corrosion processes and the behaviour of metals in different environments and conditions.

Electrochemical polarization methods. The polarization relationships, recorded potentiostatically or potentiodynamically, allow the determination of various corrosion-electrochemical parameters, such as corrosion rate, corrosion potential, pitting potential etc. Measurements were performed using an EG&G Princeton Applied Research potentiostat/galvanostat, model 263A, equipped with the specialized software package PowerCORR®. Three electrochemical methods were used: (i) Open circuit potential (OCP), measured over 1 hour; (ii) Cyclic potentiodynamic polarization method (scan rate 5.0 mV s^{-1}), (iii) Potentiostatic method [14,15].

After anodic polarization for 20 minutes, at potential 100 mV more positive than the potential of a pit nucleation, obtained potentiodynamically, by LM, SEM and EDX analyses were studied the topography and chemical content of the products on the steel surfaces.

2.2.2. Physical methods

Light microscopy (LM). The morphology of the surfaces was determined by LM, using a microscope OPTIKA® Model: B-500Bi.

Scanning electron microscopy (SEM). The morphology and structure of the surfaces were examined by scanning electron microscopy, using a SEM/FIB LYRA I XMU, TESCAN electron microscope, equipped with ultrahigh resolution scanning system secondary electron image (SEI).

Energy dispersive X-ray spectroscopy (EDX). The energy dispersive spectroscopy is a local X-ray spectral analysis, which permits qualitative and quantitative determination a content of the elements on surface micro volumes (in order of several μm^3). Apparatus Quantax 200, BRUKER with spectroscopic resolution at Mn-Ka and 1 kcps 126 eV was used.

3. Results and discussion

3.1. Relationships "Open circuit potential (OCP) – time"

The potential-time relationships taken over 1 h at 37°C, for steels Cr18Mn12N and Cr18Ni9, are presented in Fig. 2: (a) in Ringer's infusion solution and (b) in Hartmann's lactate infusion solution.

It can be seen that the course of the *potential-time* curves is similar for both steels studied. The displacement of potentials in the positive direction is an indication of the formation of a passive/shielding layer on the surface of the steels. The initial potential of Cr18Mn12N steel was about –0.25 V (SCE) and that of Cr18Ni9 was about –0.3 V (SCE) , and after one hour, the potential of the high nitrogen steel is about 30 mV more positive than that of Cr-Ni steel, in both environments studied.

Although not large, the difference in potentials of the two steels, measured in open circuit conditions, indicates that Cr18Mn12N steel, whose potential is more positive in both solutions, has better resistance. The latter is due to its higher tendency to form a surface protective film, i. e., to passivation.

3.2. Cyclic potentiodynamic polarization Relationships

In the cyclic potentiodynamic polarization method, the potential from its steady-state value is initially expanded in the anodic then reversed in the cathodic direction. The pitting nucleation potential (E_{pit}) is determined by the sharp increase in anode current when passing through the passive region. When a certain value of current is reached (10^{-4} A cm^{-2}), a reversal of the potential direction follows, after which it stabilizes and finally decreases rapidly as a consequence of the repassivation of the pittings. The intersection of the curve with that from the anode direction corresponds to the protection potential or so-called pitting repasivation potential (E_{rp}).

Fig. 3 shows cyclic potentiodynamic polarization relationships *E-lgi* taken for Cr18Mn12N and Cr18Ni9 steels from –250 mV vs. Open circuit potential (OCP) at a potential scan rate of 5.0 mV s^{-1} in Ringer's infusion and Hartmann's lactate infusion solutions, at a temperature of 37°C. The main parameters (E_{corr}, E_{pit}, E_{rp} and i_{corr}, i_{pass}), determined from the cyclic potentiodynamic polarization curves (CPPC) are presented in TABLE 4.

From the values of the measured parameters presented in the table, it can be seen that the corrosion potentials of Cr18Mn12N steel are more positive than those of Cr18Ni9 steel in both solutions, while its corrosion rates, although slightly, are higher. The i_{pass} values of the two steels are also very close. More significant is the difference in the values of E_{pit} and E_{rp}, as they are more unfavourable for high nitrogen steel.

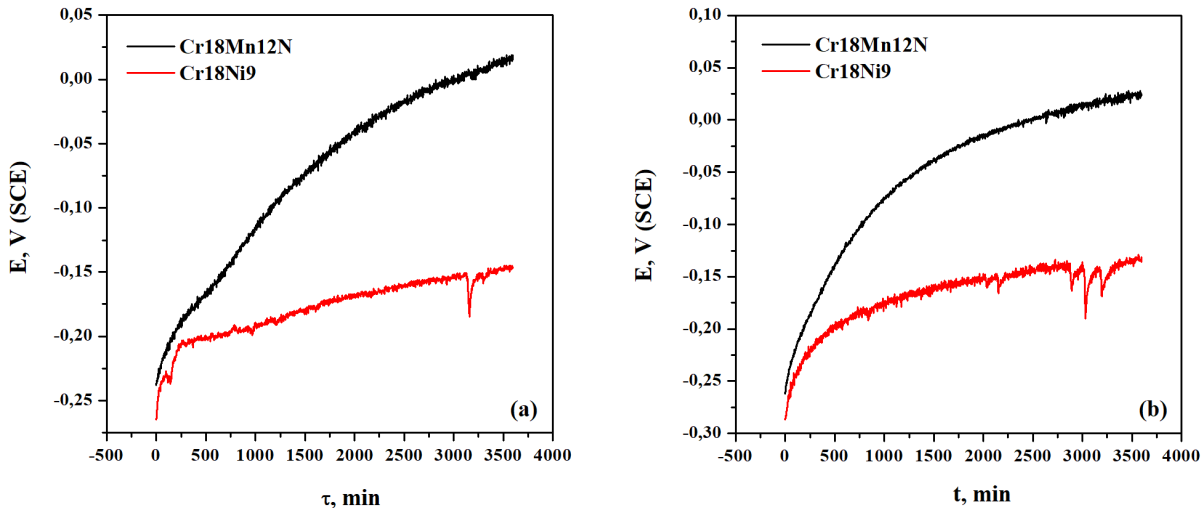

Fig. 2. Potential-time relationships taken over 1 h, at 37°C in: (a) Ringer's infusion solution and (b) Hartmann's lactate infusion solution

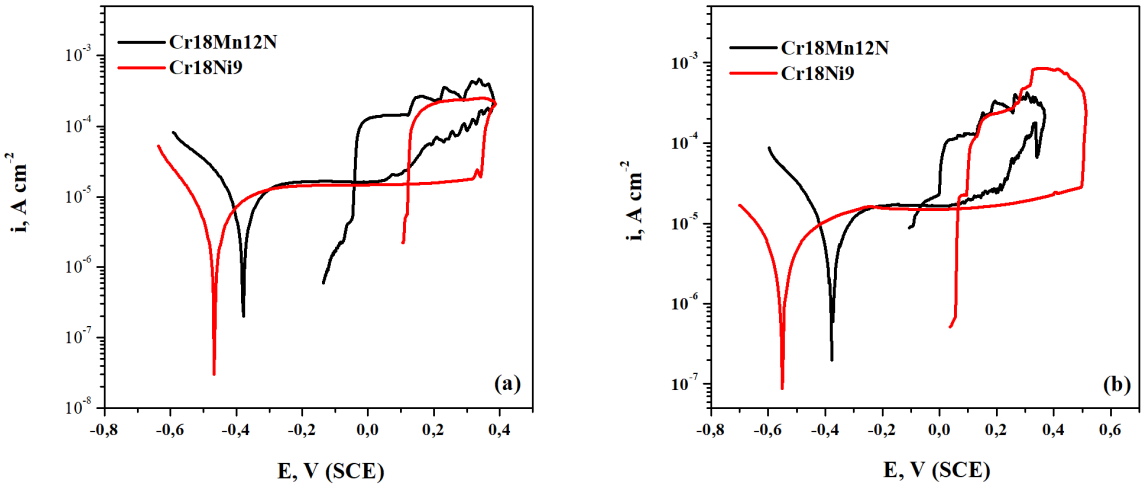

Fig. 3. Potentiodynamic polarization relationships/ dependencies for (a) Ringer's infusion solution and (b) Hartmann's lactate infusion solution obtained with 5.0 mV s^{-1}, at 37°C

TABLE 4

The parameters from CPPC

Solutions	Steels	E_{corr}, V (SCE)	E_{pit}, V (SCE)	E_{rp}, V (SCE)	i_{corr}, A cm^{-2}	i_{pass}, A cm^{-2}
Ringer's	Cr18Mn12N	–0.383	+0.060	–0.050	1×10^{-6}	0.7×10^{-5}
	Cr18Ni9	–0.470	+0.343	+0.120	9×10^{-7}	0.4×10^{-5}
Hartmann's lactate	Cr18Mn12N	–0.386	+0.223	–0.615	1.3×10^{-6}	0.8×10^{-5}
	Cr18Ni9	–0.551	+0.492	+0.069	0.2×10^{-6}	0.7×10^{-5}

3.3. Characterization of the steel surfaces by light microscopy (LM)

Light microscopy was used to establish the nature, shape and size of the corrosion damage on the surfaces of the two steels examined. Fig. 4 shows photographs of the steels exposed in the two solutions after potentiostatic polarization at a potential with 100 mV more positive than E_{pitt}, as determined from potentiodynamic studies.

Macro and many micropitting are observed on the surface of the steels, more and with larger sized are pittings on Cr18Ni9, compared to the pittings on the surface of Cr18Mn12N. The pits are irregular and spherical in shape and could be divided formally in two groups: small pits with size in the range 40-60 μm and large – with above 200 μm.

The macropits are of the closed type, irregular in shape and partially preserved crust, and around them are overlays of corrosion products and crystallized salts. These accumulations of salts and corrosion products are in the form of an ellipse, two-thirds of which surrounds the pit in a circle, and one end is drawn outwards.

3.4. Characterization of the surfaces by SEM and EDX

Scanning electron microscopy (SEM) together with X-ray spectroscopy (EDX) and the SE detector (Secondary electron emission) represent ones of the most important material science and engineering analytical techniques. The micrographs in Fig. 5 show the morphology of the surface of HNS and classical Cr-Ni stainless steel after potentiostatic polarization in Ringer's infusion solution and Hartmann's lactate infusion solution. The main form of corrosion on the steel surfaces after electrochemical treatment of the samples is pitting corrosion.

The microscopy observations indicate more numerous pits on Cr18Ni9 steel surfaces which are larger in comparison to these on the surface of the Cr18Mn12N samples in both solutions. Some of the pits are open and the others are subsurface types.

EDX analyses of the corrosion products around the pits were performed after electrochemical treatment of the samples in the two solutions. TABLE 5 summarizes the element composition in atomic and weight percentages, obtained by the EDX spectra of the corrosion products. The analysis indicates high content of O, P, Cl and other elements, which are components of the solutions, as well as Fe, Mn, Ni, Cr and so on. Therefore, apart from the oxides formation during surface dissolution there exist also metal chlorides and phosphates. The results presented in the tables indicate that the Ringer's infusion solution accordance to the Hartmann's lactate infusion solution is more aggressive to investigate steels.

4. Conclusions

In a comparative study of the corrosion behaviour of two austenitic stainless steels (Cr18Ni9 and HNS Cr18Mn12N) proposed for biomedical applications, the nature (pitting corrosion,

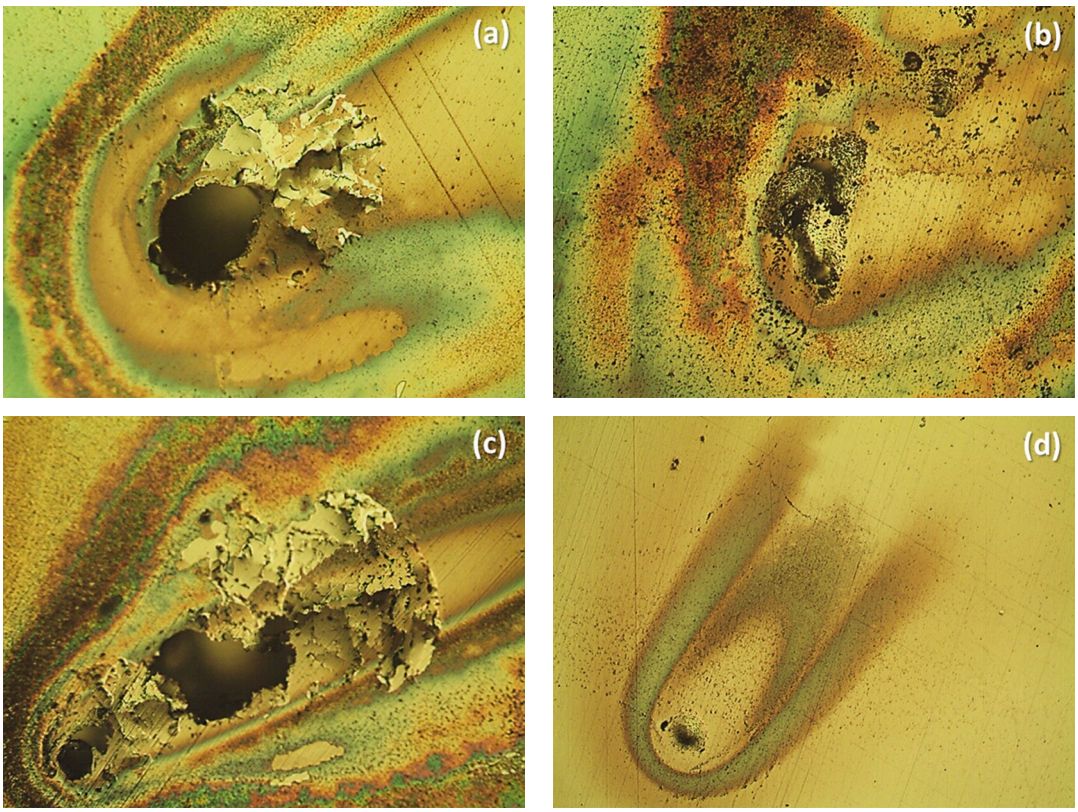

Fig. 4. LM – photographs of Cr18Ni9 and Cr18Mn12N steels after potentiostatic polarization in Ringer's infusion (a, b) and Hartmann's lactate infusion solutions (c, d), ×200

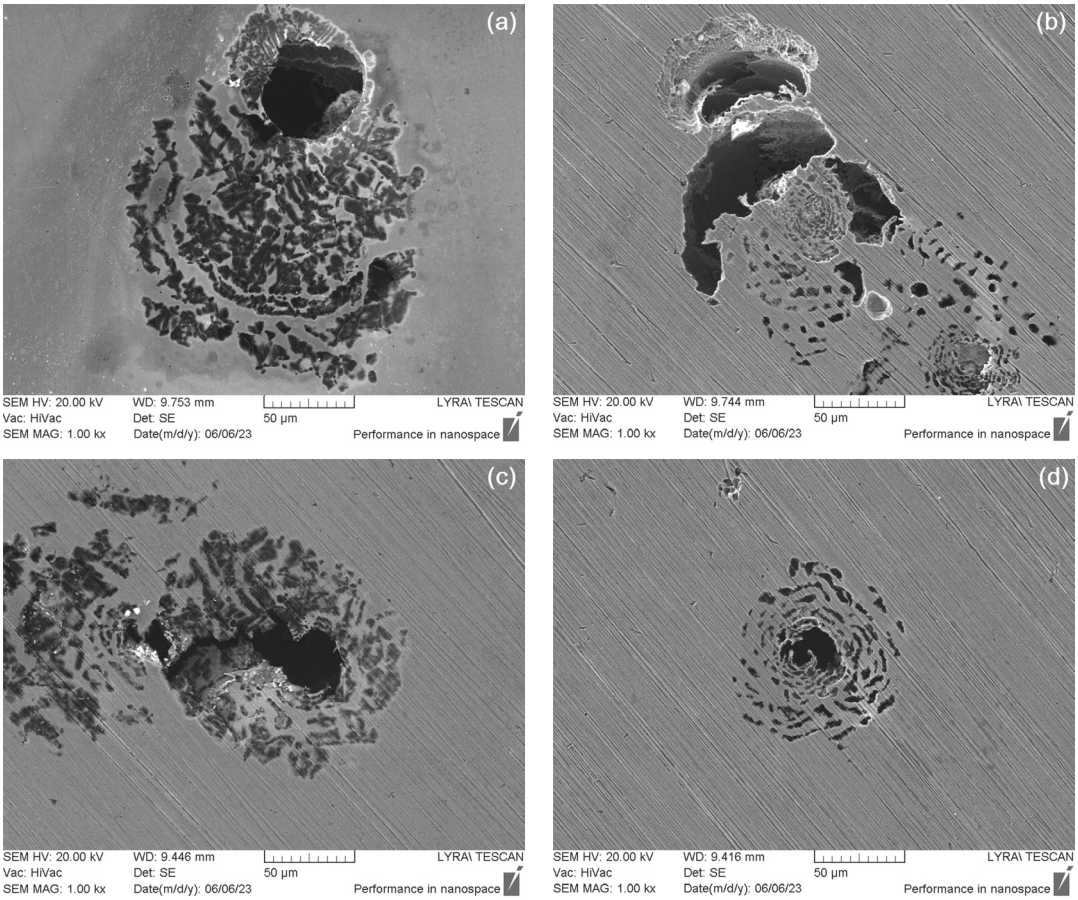

Fig. 5. SEM – microphotographs of Cr18Ni9 and Cr18Mn12N steels after potentiostatic polarization in Ringer's infusion solution (a, b) and Hartmann's lactate infusion solution (c, d)

TABLE 5

EDX analyses of the elements on the surfaces in Ringer‘s infusion solution and Hartmann’s lactate infusion solution

Solutions	Ringer’s infusion				Hartmann’s lactate infusion			
Elements	Concentration				Concentration			
	Cr18Ni9		Cr18Mn12N		Cr18Ni9		Cr18Mn12N	
	Wt. %	At. %	Wt. %	At. %	Wt. %	At. %	Wt. %	At. %
Fe	56.32	*37.49*	44.23	*24.20*	69.99	*63.81*	69.54	*65.67*
Cr	14.33	*10.24*	15.46	*9.08*	16.47	*16.13*	16.11	*16.40*
Ni	8.55	*5.42*	—	—	9.16	*7.95*	—	—
Mn	—	—	6.34	*3.53*	—	—	10.95	*10.51*
O	16.14	*37.50*	29.40	*56.14*	1.52	*3.59*	0.54	*1.27*
C	1.99	*6.16*	1.65	*4.21*	1.43	*6.05*	0.76	*3.33*
Cl	0.29	*0.30*	0.20	*0.17*	0.04	*0.05*	0.07	*0.11*
P	0.94	*1.13*	1.48	*1.46*	0.55	*1.03*	1.12	*1.53*
S	0.54	*0.63*	0.49	*0.47*	0.16	*0.26*	0.46	*0.41*
Ca	0.14	*0.13*	0.17	*0.13*	0.18	*0.23*	0.15	*0.21*
Si	0.75	*1.00*	0.58	*0.63*	0.50	*0.90*	0.30	*0.56*

with different shaped and sized pits) and likely composition of the corrosion products were determined in two model infusion solutions. The results show that nitrogen-containing steel possesses higher stability in model environments and is therefore more suitable for biomedical applications.

Acknowledgments

„This work is developed as part of contract №: BG-RRP-2.004-0002-C01, project name: BiOrgaMCT, Procedure BG-RRP-2.004 „Establishing of a network of research higher education institutions in Bulgaria“, funded by BULGARIAN NATIONAL RECOVERY AND RESILIENCE PLAN“.

REFERENCES

[1] T.S. Hin, Engineering materials for biomedical applications. World Scientific Publishing Co. Pte. Ltd., Toh Tuck Link, Singapore, 2004.

[2] A.C. Fraker, in ASM Handbook, vol. 13, ASM International, USA, 1987, p. 3313.

[3] M. Li, T. Yin, Y. Wang, F. Du, X. Zou, H. Gregersen, G. Wang, Study of biocompatibility of medical grade high nitrogen nickel-free austenitic stainless steel in vitro. Mater. Sci. Eng. C **43**, 641-648, (2014). DOI: https://doi.org/10.1016/j.msec.2014.06.038

[4] S. Virtanen, I. Milosev, E. Gomez-Barrena, R. Trebse, J. Salo, Y.T. Konttinen, Special modes of corrosion under physiological and simulated physiological conditions. Acta Biomater. **4** (3), 468-476 (2008). DOI: https://doi.org/10.1016/j.actbio.2007.12.003

[5] G.E. Novikova, Introduction to corrosion of bioimplants. Prot. Met. Phys. Chem. Surf. **47**, 372-380 (2011). DOI: https://doi.org/10.1134/S2070205111030105

[6] R. Simitchiiska, D. Ivanova, L. Fachikov, SEM and EDX Study of Stainless Steels, Suggested as Human Body Implants. IOP Conf. Series: Materials Science and Engineering **374**, 012002 (2018). DOI: https://doi.org/10.1088/1757-899X/374/1/012002

[7] M.S. Baltatu, M.C. Spataru, L. Verestiuc, V. Balan, C. Solcan, A. V. Sandu, V. Geanta, I. Voiculescu, P. Vizureanu, Design, Synthesis, and Preliminary Evaluation for Ti-Mo-Zr-Ta-Si Alloys for Potential Implant Applications. Materials **14**, 6806 (2021). DOI: https://doi.org/10.3390/ma14226806

[8] M.-C. Spataru, F.D. Cojocaru, A.V. Sandu, C. Solcan, I.A. Duceac, M.S. Baltatu, I. Voiculescu, V. Geanta, P. Vizureanu, Assessment of the Effects of Si Addition to a New TiMoZrTa System. Materials **14**, 7610 (2021). DOI: https://doi.org/10.3390/ma14247610

[9] J. Zhao, M. Haowei, A. Saberi, Z. Heydari, M.S. Baltatu, Carbon Nanotube (CNT) Encapsulated Magnesium-Based Nanocomposites to Improve Mechanical, Degradation and Antibacterial Performances for Biomedical Device Applications. Coatings 1**2**, 1589 (2022). DOI: https://doi.org/10.3390/coatings12101589

[10] M. Sumita, T. Hanawa, S.H. Teoh, Development of nitrogen-containing nickel-free austenitic stainless steels for metallic biomaterials-review. Mater. Sci. Eng. C **24** (6-8), 753-760 (2004). DOI: https://doi.org/10.1016/j.msec.2004.08.030

[11] N. Hassan, N.A. Abdel Ghany, Corrosion of biomaterials: anodic treatment and evaluation of 316L stainless steel in simulated body fluid, Corrosion Engineering, Science and Technology **52** (4), 267-275 (2017). DOI: https://doi.org/10.1080/1478422X.2016.1267932

[12] Q. Chen, G.A. Thouas, Metallic implant biomaterials. Mater. Sci. Eng. R **87**, 1-57 (2015). DOI: https://doi.org/10.1016/j.mser.2014.10.001

[13] L. Benea, L. Dragus, D. Mocanu, Corrosion Assessment of Nickel – Base – Dental Alloys in Ringer Biological Solution Studied by Electrochemical Techniques. Arch. Metall. Mater. **67** (2), 529-533 (2022). DOI: https://doi.org/10.24425/amm.2022.137786

[14] ISO/FDIS 17475, 2005.

[15] ASTM G61-86, 2003.